Available online at www.sciencedirect.com
SCIENCE DIRECT®
Thin Solid Films 447–448 (2004) 436–442
www.elsevier.com/locate/tsf

Effect of substrate bias voltage on amorphous Si–C–N films produced by PVD techniques

L. Cunha[a,]*, C. Moura[a], J. Leme[a], G. Andrês[a], K. Pischow[b]

[a]*Physics Department, University of Minho, Campus de Gualtar, Braga 4710-057, Portugal*
[b]*Savcor Coatings Oy, Insinöörinkatu 7, FIN-50100, Mikkeli, Finland*

Abstract

$Si_xC_yN_z$ thin films were deposited by reactive magnetron sputtering on glass and steel substrates. The films were grown in a rotation mode over a carbon and a silicon targets in a mixed Ar/N_2 atmosphere. The substrates were held at a substrate temperature of 573 K. The argon flow was kept constant (100 sccm) and the nitrogen flow was 20 sccm or 25 sccm, in each one of the two series of produced films, resulting in a working pressure at approximately 0.5 Pa. The substrate bias varied between grounded and −100 V. The films were analysed with respect to microstructure, state of chemical bonding and optical properties by X-ray diffraction (XRD), Raman spectroscopy (RS), optical reflectance and transmittance. Raman spectroscopy was used as a probe of microstructural modifications induced by deposition conditions. The main features observed in RS spectra are the well-known D- and G-bands characteristic of amorphous carbon materials. The position, widths and intensity ratio of these bands are found to be dependent of the films deposition conditions. The refractive index, absorption coefficient, optical band gap and also the thickness were calculated from transmittance spectra obtained between 200 and 2500 nm. The residual stress of the coatings depends on deposition conditions and was calculated by measuring the substrate curvature before and after film deposition. The curvature of the samples was measured by laser triangulation in two series of two orthogonal directions. All coatings were in a state of compressive residual stress. The average hardness and Young's modulus of the produced coatings is approximately 16 GPa and 170 GPa, respectively. The nano-hardness of the grounded produced samples presented values approximately 30% lower.

Keywords: Magnetron sputtering; Young's modulus; Nano-indentation experiments; Raman spectroscopy; Si–C–N films

1. Introduction

Wear resistance and corrosion protection are required in many tribological applications. There are many studies and research on ceramic hard coatings, but Si–C–N systems have not been extensively studied. The production of ternary system Si–C–N could exhibit interesting properties, in combining the characteristics of binary compounds—C_3N_4, Si_3N_4 and SiC.

Theoretical calculations predict that α- and β-C_3N_4 may present hardness and bulk modulus similar of diamond [1–4], but the synthesis of crystalline carbon nitride is difficult to achieve, but some attempts have been made. The incorporation of some silicon in the growth of carbon nitride films by microwave plasma-enhanced CVD promoted the formation of crystallites [5], although an excess of Si incorporation led to the formation of amorphous phase in PVD process [6]. The growth of ZrN/CN_x super-lattices with carbon nitride (nitride to carbon ratio of 1:3) ultra thin layers (<2 nm) presented some crystalline regions [7] with sp^3 bond states. Silicon nitride (Si_3N_4) is a well-known material: high hardness; high fracture toughness; wear resistance; high thermal stability; chemical inertness; and good insulating properties [8–10]. It is a good material for applications in which wear resistance at high temperature is required and in corrosive environments. In consequence of its dielectric properties, silicon nitride is also used for optical and electronic industry. The dielectric properties are strongly dependent on composition. The optical band-gap in SiN_x changes from 1.8 to 5 eV when x changes from 0 to 1.7. Silicon carbide (SiC) has also interesting properties: hard

---

*Corresponding author. Tel.: +351-253-604-066; fax: +351-253-678-981.
E-mail address: lcunha@fiscia.uminho.pt (L. Cunha).

0040-6090/04/$ - see front matter © 2003 Elsevier B.V. All rights reserved.
doi:10.1016/S0040-6090(03)01121-0

Table 1
Deposition parameters and properties of $Si_xC_yN_z$ films, growth rate (Z), density (ρ), thickness (t_c), hardness (*H*), Young's modulus (*E*) and residual stress (σ)[a]

V_{subs} [*V*]	Samples prepared with Φ (N_2) = 20 sccm and P_{Si} = 100 W						Samples prepared with Φ (N_2) = 25 sccm and P_{Si} = 150 W					
	Z [nm/min] (*T*/*BC*)	ρ [g/cm^3] (*T*/*BC*)	t_c [μm] (*T*/*BC*)	*H* [GPa]	*E* [GPa]	σ [GPa]	Z [nm/min] (*T*/*BC*)	ρ [g/cm^3] (*T*/*BC*)	t_c [μm] (*T*/*BC*)	*H* [GPa]	E [GPa]	σ [GPa]
0	2.7/2.7	1.5/1.4	1.3/1.3	10.2	112.1	−0.9	3.4/4.6	2.8/2.1	1.6/2.2	11.0	124.0	−0.8
−25	2.7/2.0	2.1/2.9	1.3/1.0	15.7	164.1	−2.0	4.1/2.7	2.0/3.0	2.0/1.3	15.8	168.2	−1.3
−50	3.4/2.5	2.0/2.5	1.6/1.2	17.4	179.1	–	3.1/3.4	2.0/1.9	1.5/1.6	16.5	165.9	−1.6
−75	2.9/2.7	2.0/2.2	1.4/1.3	18.0	189.2	–	3.5/1.9	2.6/4.7	1.7/1.0	16.4	179.4	–
−100	2.9/2.7	1.6/1.7	1.4/1.3	18.9	200.7	–	3.7/2.7	2.2/3.1	1.8/1.3	18.2	192.3	–

[a] The *T* values were obtained for glass substrate samples using data obtained from transmittance spectra. The *BC* values were obtained for steel substrates samples, using data obtained from ball cratering measurements.

ceramic; resistant to chemically aggressive environments; wear resistant; presents high thermal conductivity [8,11–13]; and low thermal expansion. Silicon carbide is also an indirect semiconductor with wide energy band-gap (2.4–3.4 eV depending on polytype) [14].

In films containing carbon, the increase of the hardness is strongly correlated with the sp^3 (only σ bonds) concentration in the film [15]. Besides hardness, low surface energy is also important in order to avoid sticking effects, mainly in plastic processing. To achieve this effect, low surface energy is required. In the case of carbon, low surface energy may be achieved by promoting sp^3-bonding states, reducing the amount of unsatured bonds.

Most of the published work about production of Si–C–N refers to high temperature deposition processes (CVD). High temperature deposition (typically between 600 and 1200 °C) is a strong limitation for industrial applications. Only few works has been published about the synthesis of Si–C–N at low growth temperatures. Pulsed laser deposition (PLD) was used by some authors [16,17], but there is some work published with ion sputtered deposition of carbon and silicon in a nitrogen atmosphere, with simultaneous nitrogen ion bombardment of substrates [18] and reactive magnetron sputtering [19–22].

In the present work, it reports the deposition and characterization of Si–C–N coatings on glass and steel substrates. The effect of negative substrate d.c. bias is studied, using non-destructive RS and optical transmittance. In fact, an understanding of the local chemical bonding is necessary to optimise the growth parameters for improvement of the physical properties. The investigation of the structural arrangements is not straightforward since five types of bonds between silicon, carbon and nitrogen are present in this disordered material. Moreover, the ability of carbon to present sp^2 or sp^3 coordination adds some complexity to the bonding states.

2. Sample preparation and experimental techniques

The samples were deposited by reactive r.f. magnetron sputtering, in a rotation mode (4 rev./min) from high purity C and Si targets, onto polished stainless steel (AISI 316), to measure mechanical properties and glass substrates, to measure optical properties. The depositions took place in an Ar/N_2 atmosphere using an Alcatel SCM650 apparatus. Prior to all depositions, the substrates were ultrasonically cleaned and sputter etched with 200 W r.f. power for 10 min in a 0.4 Pa argon atmosphere. During all depositions some parameters were kept constant: the r.f. power applied to the carbon target (500 W $\Leftrightarrow$ 1.6 W/cm^2), the substrate temperature (300 °C), the targets to substrate distance (65 mm) and the argon flow (100 sccm). A set of samples (set A) was prepared with a nitrogen flow of 20 sccm and a 100 W r.f. power applied to the silicon target (2.3 W/cm^2). During deposition, five different substrate d.c. bias were applied (from grounded to −100 V). The second set of films (set B) was prepared with the same variation of the substrate bias, but the nitrogen flow was 25 sccm and the silicon target power was 150 W (3.4 W/cm^2). The total pressure during experiments was approximately 0.5 Pa. The summary of the deposition parameters is shown in Table 1.

The ball cratering technique was used to measure the thickness of the coatings deposited on steel substrates (thickness BC in Table 1). The hardness and Young's modulus were measured perpendicularly to the surface by nanoindentation with a microprobe equipped with a Berkovich diamond indenter (Nanoindenter XP), using the method of Oliver and Pharr [23]. The load measurement resolution was 1 μN. The instrumented indentation depths were 100 nm and they were achieved with average loads between 2.245 and 4.069 mN. The nanohardness and Young's modulus values were achieved by calculating the average of the results obtained by 20 indentations in each film.

The residual stress of the coatings was calculated using Stoney's equation [24] after measuring the parabolic deflection of the substrate by laser triangulation. The residual stress values were obtained by calculating the average of the measurements calculated in two series of two perpendicular directions.

The transmittance spectra were obtained in a Shimadzu UV-3101PC spectrophotometer, in a wavelength range between 200 and 2500 nm. The spectra were obtained in 2-nm steps and the slit width was 2 nm. These spectra were used to obtain the thickness of the samples deposited on glass (thickness *T* in Table 1), the refractive index and absorption coefficient were calculated using Swanepoel method [25]. The transmittance spectra of amorphous films also allowed the calculation of the optical band gap by the Tauc method [26,27].

Coatings density was estimated from the mass gain of the samples during deposition divided by the volume of the film (deposited area multiplied by film thickness). Table 1 shows two density values for each film (*T* and *BC*): the density *T* is estimated by using the film thickness obtained by transmittance spectra for glass substrate samples. The density *BC* is estimated by using film thickness measured by ball cratering for steel substrate samples.

The Raman scattering analysis of different films has been performed at room temperature using the 488 nm line of an argon ion laser. The measurements were performed with a BHSM Olympus microscope using ×100 MS Plan objective. To limit local heating of the sample the power of incident light onto the sample was 2.5 mW. The scattered light was detected by a triple monochromator Jobin Yvon T64000 coupled to a CCD detector. The spectra have been recorded over a very wide frequency range (200–2500 cm^{-1}).

The structure analyses were made after X-ray diffraction (XRD), using Cu Kα radiation in a θ–2θ set-up.

This study will show the variation of some physical properties and microstructure of the Si–C–N films with the substrate bias.

3. Results and discussion

In order to characterize the deposited films, we have performed Raman spectroscopy since this is a powerful non-destructive technique that can be used to characterize the sp^2-bonded and sp^3-bonded carbon, since Raman scattering is directed correlated with changes in microstructure. It is also known that the G-band is sensitive to deposition conditions such as composition, pressure and bias voltage.

The first-order phonon modes of diamond and graphite occur at well-separated frequencies of 1332 cm^{-1} and 1580 cm^{-1}, respectively. In amorphous materials, the lack of long-range order leads to a relaxation of the *k*-selection rules governing the Raman process, and all vibrational modes can participate in RS. In disordered graphite two peaks are present: the G-peak at approximately 1580–1600 cm^{-1} and the D-peak at approximately 1350 cm^{-1} [28].

The Raman spectrum obtained for all the samples are composed of broad features characteristic of the amorphous nature of the films, confirmed by XRD, and dominated by intense and asymmetric bands in the region between 900 and 1900 cm^{-1} due to a highly overlapping of the well known G-band centred at approximately 1540 cm^{-1} and D-band centred at approximately 1400 cm^{-1} associated with disordered–allowed zone edge modes of disordered graphitic carbon, that become Raman active due to the lack of long-range order. In all registered spectra less intense structures are detected. In the low frequency range, the band located at approximately 750 cm^{-1}, is attributed to optical-like modes of hetero-polar Si–C bonds. In the high frequency range, the band located at approximately 2200 cm^{-1}, is ascribed to C≡N vibrations.

In order to analyse qualitatively the Raman scattering, each spectrum was fitted with an asymmetric Breit–Wigner–Fano (BWF) line shape, to the G-Band, which is described by the Eq. (1) [29,30]:

$$I(\omega)=\frac{I_0\left[1+2(\omega-\omega_0)/Q\Gamma\right]^2}{1+\left[2(\omega-\omega_0)/\Gamma\right]^2} \tag{1}$$

where $I(\omega)$ is the calculated Raman intensity, $\omega_{0,}$ I_0 and Γ are the peak positions, the intensity and full with at half maximum (FWHM), respectively, Q is BWF coupling factor. To fit the D-band, a Lorentzian line shape was used. It has been shown that the parameter which is sensitive to the sp^3 fraction of the films is the Q factor, on the BWF adjustment, that measures the 'skewness' of the peak [30]. Films with high sp^3 content have more symmetrical peaks and thus large (negative) values of Q. In consequence, the evaluation of the Q factor is an indirect method to infer the sp^3/sp^2 fraction of the films.

In Fig. 1a it reports on the variation of the Q factor with substrate bias for two kinds of samples. It is clear that the Q factor decreases with the increase of the substrate bias. This behaviour can be understood as an increase of the sp^3 fraction in the films, due to an increase of the C–C and C–N sp^3 coordination, and consequently, a decrease in sp^2 content. It is also known that when the C amount decreases the G-band becomes more symmetrical [28].

Fig. 2a and b shows the G- and D-band positions and their relative intensity (I_D/I_G) as a function of substrate bias voltage. It can be seen from Fig. 2a that both the D- and the G-bands positions shift to upper and lower frequencies, respectively, with the increase of the negative bias voltage. These shifts are more pronounced for

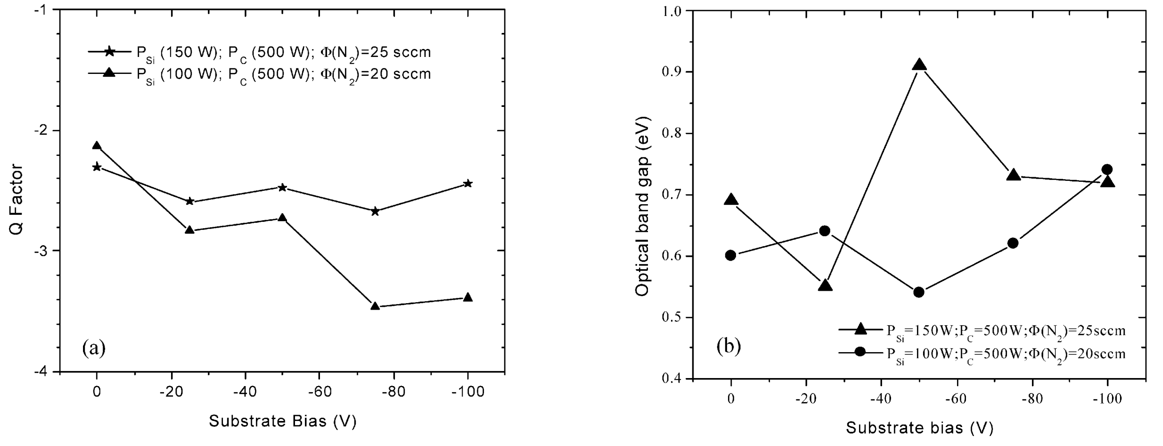

Fig. 1. (a) The Q factor extracted from the BWF fits to Raman spectra as a function of substrate bias voltage. (b) Optical band gap of $Si_xC_yN_z$ films calculated from transmittance spectra as a function of substrate bias.

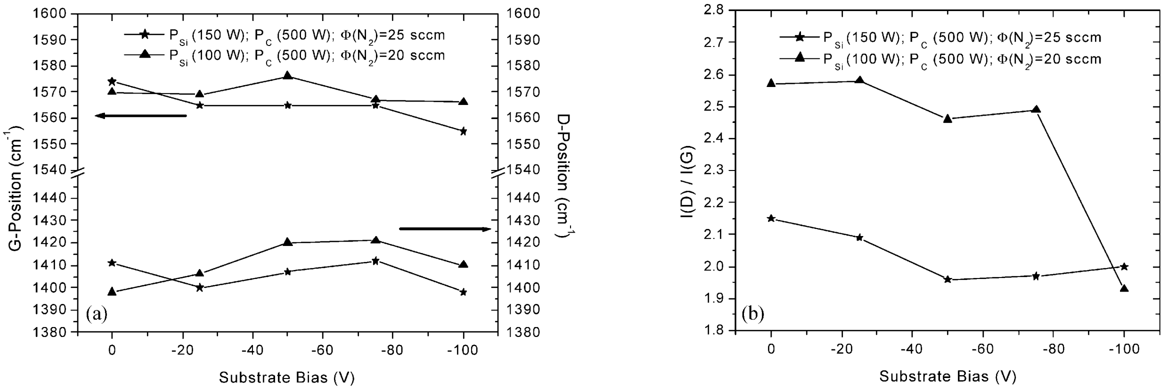

Fig. 2. (a) G and D peak position (b) relative intensity ratio of D and G peaks (I_D/I_G) as a function of substrate bias.

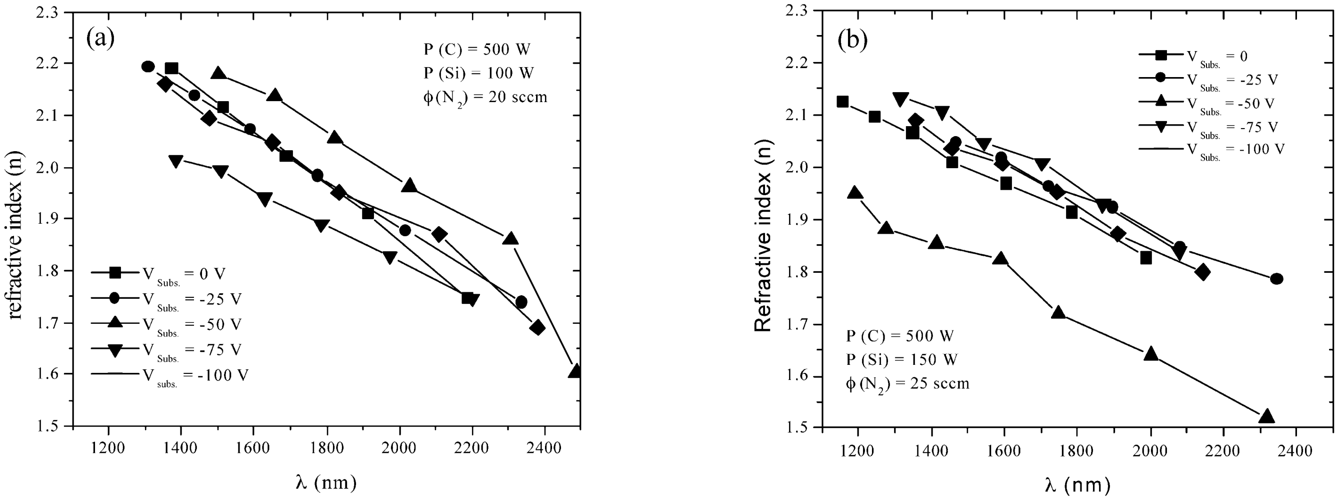

Fig. 3. Refractive index of $Si_xC_yN_z$ films calculated from transmittance spectra as a function of wavelength.

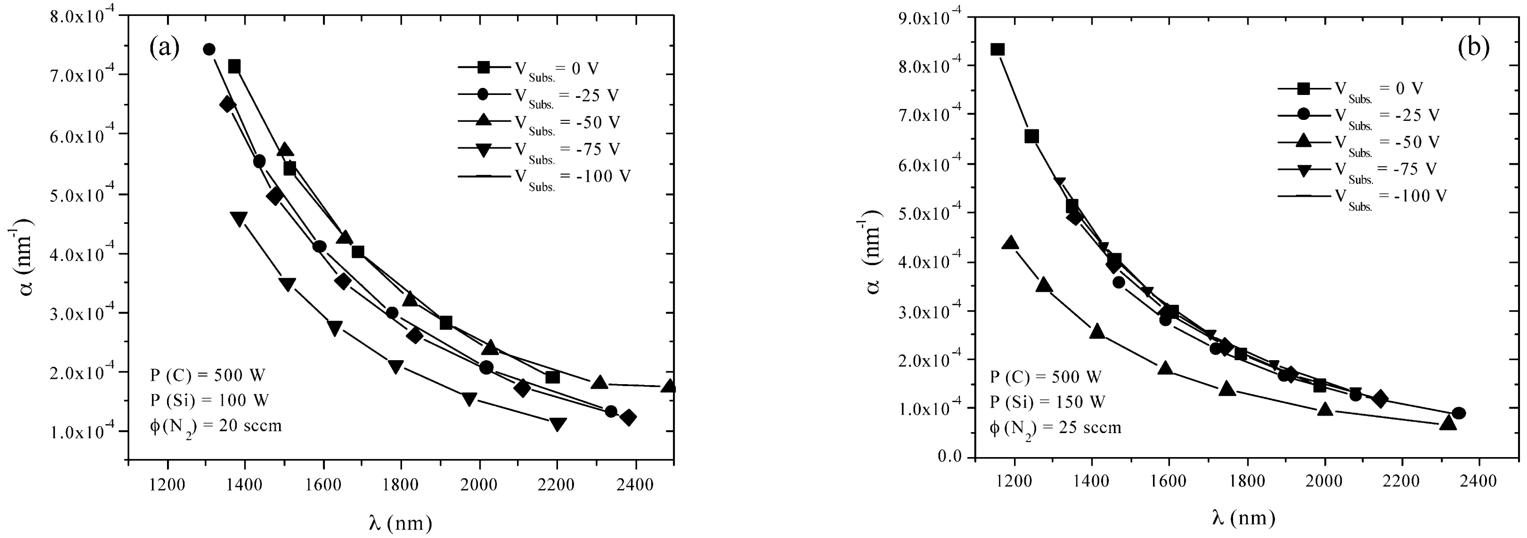

Fig. 4. Absorption coefficient of $Si_xC_yN_z$ films calculated from transmittance spectra as a function of wavelength.

films deposited with higher power applied to the silicon target. Excepting the films produced with grounded substrate, the G- and D-bands appear at lower frequencies for the films deposited with higher power applied to Si target. From Fig. 2b we can see that the intensity ratio decreases as the bias voltage increase. This behaviour is correlated with an increase of the ratio sp^3/sp^2. In fact the simultaneous shift of both bands and the decrease in the relative intensity can be explained by the incorporation of Si atoms on the network, promoting the increase in sp^3 bonding. These observations may be correlated with the density, hardness and Young's modulus.

In general, the coatings deposited on steel substrates are denser because of ion bombardment during deposition, caused by the negative d.c. bias. The coatings produced with grounded bias present the lowest hardness and Young's modulus values. The dependence of these mechanical properties with the substrate bias may be seen in Table 1. A general increase is obtained when the negative bias increases. This is an expected result, caused by a higher compactness of the films, due to the higher ion bombardment during deposition. This increase in hardness may be related with the increase of sp^3 C–N bonding states [31], confirming the results from Raman spectroscopy. There is also some published work referring a relation between the increase of C–C sp^3 bonding states in DLC coatings with higher hardness [32,33]. We believe that in general, and within the limits of the experimental work reported in this paper, ion bombardment promotes the sp^3 bonding states provoking also an increase of hardness and Young's modulus of the Si–C–N coatings. Excluding the samples produced with grounded substrate, the average hardness and Young's modulus of the coatings are approximately 17 GPa and 180 GPa, respectively. The variation of these mechanical properties is similar for both sets of films.

The residual stress values could not be obtained for all the samples because those deposited with higher bias values demonstrated low adhesion and it was not possible to apply the bending plates method. Table 1 demonstrates an increase of compressive residual stress with increasing negative substrate bias until -50 V. This is a consequence of the ion bombardment during deposition. The high stress states also mean a high percentage of sp^3 C–N and C–C bonding states [32–34].

Our previous work showed that the refractive index has a tendency to decrease when the N_2 flow increases [22]. The results concerning the variation of the substrate bias shows that generally the refractive index of these films is similar, varying between a maximum of 2.2 and a minimum of 1.6 when the wavelength of incident radiation varies from 1200 and 2500 nm (Fig. 3). Curiously, there is an inversion of the behaviour for the samples produced with -50 V substrate bias of each set of coatings. The refractive index values of the sample of set A [$\Phi(N_2)=20$ sccm and $P_{Si}=100$ W], are the highest of the set and that of set B [$\Phi(N_2)=25$ sccm and $P_{Si}=150$ W) are the lowest.

The absorption coefficient of the Si–C–N coatings, when the wavelength of incident radiation varies from 1200 and 2500 nm, presents also similar behaviour. Therefore, the higher values were obtained for the grounded substrate produced samples (Fig. 4).

The highest optical band gap was obtained for the sample produced higher nitrogen flow, higher power applied to Si target and with -50 V substrate bias (0.91 eV), the other samples have similar values (average 0.64 eV) but it seems that there is a tendency to an increase of the band gap with the increase of the substrate bias (Fig. 1b). The optical band gap is an indirect proof of the ratio sp^3/sp^2 bonding states [35,36]. Low optical band gap values correspond to big graphitic clusters and low sp^3/sp^2 ratios [30,37]. The obtained results show a little increase of the sp^3 bonding states, meaning a lower surface energy, with the increase of substrate bias.

4. Conclusion

The analyses of the $Si_xC_yN_z$ thin films produced by r.f. reactive magnetron sputtering showed the following results:

- Raman spectroscopy has been used to study the effects of deposition parameters of the films. The results show that the changes in the relative intensity of the D and G bands with a simultaneous shift in the band's position can be correlated as a signature of mixed sp^2 and sp^3 coordination of carbon in a disordered network. These results support the increases of hardness (average 16 GPa), Young's modulus (average 170 GPa) and compressive residual stress (average 1.3 GPa) of the produced films, caused by the increase of ion bombardment during deposition. The samples produced with grounded substrate have significantly lower values.
- The refractive index is between 1.6 and 2.2. The behaviour of the refractive index in function of wavelength of incident radiation is similar for all the produced samples.
- The order of magnitude of the absorption coefficient for all the samples produced is 10^{-4} nm^{-1}. The samples produced with grounded substrate presented higher values.
- The optical band gap is approximately 0.64 eV, but in general, higher values are obtained for the samples produced with $\Phi(N_2)=25$ sccm and $P_{Si}=150$ W.
- X-Ray diffraction patterns confirmed the amorphous nature of the produced films.

Acknowledgments

The authors gratefully acknowledge Mr Massoun Atfeh, from Savcor Coatings Oy (Finland) for help in obtaining XRD data and nanoindentation measurements.

References

[1] S. Boughaba, G.I. Sproule, J.P. McCaffrey, M. Islam, M.J. Graham, Thin Solid Films 402 (2002) 99.
[2] A.Y. Liu, M.L. Cohen, Science 245 (1989) 841.
[3] A.Y. Liu, M.L. Cohen, Phys. Rev. B41 (1990) 10727.
[4] C.-M. Sung, M. Sung, Mater. Chem. Phys. 43 (1996) 1.
[5] L.C. Chen, C.K. Chen, D.M. Bhusarim, K.H. Chen, Y.C. Jong, D.Y. Lin, C.F. Li, Y.S. Huang, Mater. Res. Soc. Symp. Proc. 468 (1997) 31.
[6] L.C. Chen, C.T. Wu, J.-J. Wu, K.H. Chen, Int. J. Mod. Phys. B 14 (2–3) (2000) 333.
[7] M.L. Wu, M.U. Guruz, V.P. Dravid, Y.W. Chung, S. Anders, F.L. Jr. Freire, G. Mariotto, Aool. Phys. Lett. 76 (2000) 2692.
[8] N.S. Jacobson, E.J. Opila, D.S. Fox, J.L. Smialek, Mater. Sci. Forum 251–254 (1997) 817.
[9] F.-L. Riley, J. Am. Ceram. Soc. 83 (2000) 245.
[10] M.J. Hoffman, Mater. Res. Soc. Bull. 20 (1995) 28.
[11] S.S. Shinozaki, Mater. Res. Soc. Bull. 20 (1995) 42.
[12] V.D. Krstic, Mater. Res. Soc. Bull. 20 (1995) 46.
[13] H. Matsunami, in: K.J. Klabunde (Ed.), Thin Film from Free Atoms and Particles, Academic Press, Orlando, FL, 1985, p. 301.
[14] W.J. Choyke, G. Pensl, Mater. Res. Soc. Bull. 22 (1997) 25.
[15] E. Riedo, F. Comim, J. Chevrier, A.M. Bonnot, J. Appl. Phys. 88 (2000) 4365.
[16] T. Thärigen, G. Lippold, V. Riede, M. Lorenz, K.J. Koivusaari, D. Lorenz, S. Mosch, P. Grau, R. Hesse, P. Streubel, R. Szargan, Thin Solid Films 348 (1999) 103.
[17] R. Machorro, E.C. Samano, G. Soto, L. Cota, Appl. Surf. Sci. 127–129 (1998) 564.
[18] Z. He, G. Carter, J.S. Collignon, Thin Solid Films 283 (1996) 90.
[19] S. Komatsu, Y. Hirohata, S. Fukuda, T. Hino, T. Yamashina, T. Hata, K. Kusakabe, Thin Solid Films 193–194 (1990) 917.
[20] L.C. Chen, H.Y. Lin, C.S. Wong, K.H. Chen, S.T. Lin, Y.C. Yu, C.W. Wang, E.K. Lin, K.C. Ling, Diamond Relat. Mater. 8 (1999) 618.
[21] T. Berlind, N. Hellgren, M.P. Johansson, L. Hultman, Surf. Coat. Technol. 141 (2001) 145.
[22] C. Moura, L. Cunha, H. Órfão, K. Pischow, J. De Rijk, M. Rybinski, D. Mrzyk, Surf. Coat. Technol. in press (2003).
[23] W.C. Oliver, G.M. Pharr, J. Mater. Res. 7 (1992) 1564.
[24] G.G. Stoney, Proc. R. Soc. (Lond.) A 82 (1909) 172.
[25] R. Swanepoel, J. Phys. Sci. Instrum. 18 (1983) 1214.
[26] J. Tauc, R. Grigorovici, A. Vancu, Phys. Status Solidi 15 (1966) 627.
[27] J. Tauc, in: F. Abeles (Ed.), Optical Properties of Solids, North Holland, Amsterdam, 1972.
[28] A. Chehaidar, R. Carles, A. Zwick, C. Meunier, B. Cros, J. Durand, J. Non-Cryst. Solids 169 (1994) 37.
[29] S. Prawer, K.W. Nugent, Y. Lifshitz, G.D. Lempert, E. Grossman, J. Kulik, I. Avigal, R. Kalish, Diamond Relat. Mater. 5 (1996) 433–438.
[30] A.C. Ferrari, J. Robertson, Phys. Rev. B 61 (2000) 20.
[31] H.-S. Jung, H.-H. Park, Diamond Relat. Mater. 11 (2002) 1205.
[32] S. Uhlmann, T. Frauenheim, Y. Lifshitz, Phys. Rev. Lett. 81 (1998) 641.
[33] D.R. McKenzie, D. Muller, B.A. Pailthorpe, Phys. Rev. Lett. 67 (1991) 773.
[34] E.G. Gerstner, P.B. Lukins, D.R. McKenzie, D.G. McCulloch, Phys. Rev. B 54 (1996) 20.
[35] M.A. Tamor, W.C. Vassel, J. Appl. Phys. 76 (1994) 3823.
[36] J. Robertson, E.P. O’Reilly, Phys. Rev. B 35 (1987) 2946.
[37] J. Robertson, Surf. Coat. Technol. 50 (1992) 185.